GEORG-AUGUST-UNIVERSITÄT
GÖTTINGEN

Institut für Numerische und Angewandte Mathematik

Minimization and Maximization Versions of the Quadratic Traveling Salesman Problem

Aichholzer, O., Fischer, A., Fischer, F., Meier, J.F., Pferschy, U., Pilz, A., Stanek, R.

Nr. 1

Preprint-Serie des
Instituts für Numerische und Angewandte Mathematik
Lotzestr. 16-18
D - 37083 Göttingen

Minimization and Maximization Versions of the Quadratic Traveling Salesman Problem**

Oswin Aichholzer* Anja Fischer† Frank Fischer‡
J. Fabian Meier§ Ulrich Pferschy¶ Alexander Pilz‖
Rostislav Staněk¶

Abstract

The traveling salesman problem (TSP) asks for a shortest tour through all vertices of a graph with respect to the weights of the edges. The symmetric quadratic traveling salesman problem (SQTSP) associates a weight with every three vertices traversed in succession. If these weights correspond to the turning angles of the tour, we speak of the angular-metric traveling salesman problem (Angle TSP).

In this paper, we first consider the SQTSP from a computational point of view. In particular, we apply a rather basic algorithmic idea and perform the separation of the classical subtour elimination constraints on integral solutions only. Surprisingly, it turns out that this approach is faster than the standard fractional separation procedure known from the literature. We also test the combination with strengthened subtour elimination constraints for both variants, but these turn out to slow down the computation.

Secondly, we provide a completely different, mathematically interesting MILP linearization for the Angle TSP that needs only a linear number of additional variables while the standard linearization requires a cubic one. For medium sized instances of a variant of the Angle TSP this formulation yields reduced running times. However, for larger instances or pure Angle TSP instances the new formulation takes more time to solve than the known standard model.

Finally, we introduce MaxSQTSP, the maximization version of the quadratic traveling salesman problem. Here it turns out that using some of the stronger subtour elimination constraints helps. For the special case of the MaxAngle TSP we can observe an interesting geometric property if the number of vertices is odd. We show that the sum of inner turning angles in an optimal solution always equals π. This implies that the problem can be solved by the standard ILP model without producing any integral subtours. Moreover, we give a simple constructive polynomial time algorithm to find such an optimal solution. If the number of vertices is even the optimal value lies between 0 and 2π and these two bounds are tight, which can be shown by an analytic solution

*oaich@ist.tugraz.at. Institute for Software Technology, Graz University of Technology, Inffeldgasse 16B/II, A-8010 Graz, Austria

†anja.fischer@mathematik.uni-goettingen.de. Institute for Numerical and Applied Mathematics, University of Göttingen, Lotzestrasse 16-18, D-37083 Göttingen, Germany

‡frank.fischer@uni-kassel.de. Institute for Mathematics, University of Kassel, Heinrich-Plett-Strasse 40, D-34132 Kassel, Germany

§brief@fabianmeier.de. Continentale Krankenversicherung a.G., Ruhrallee 96, D-44139 Dortmund, Germany

¶{pferschy, rostislav.stanek}@uni-graz.at. Department of Statistics and Operations Research, University of Graz, Universitaetsstrasse 15, A-8010 Graz, Austria

‖alexander.pilz@inf.ethz.ch. Institute of Theoretical Computer Science, ETH Zürich, Universitätsstrasse 6, CH-8092 Zurich, Switzerland

**A 4-pages extended abstract containing some of the results presented in this paper (without proofs) was submitted to the CTW 2016.

for a regular n-gon.

Keywords: Traveling Salesman Problem, Subtour Elimination Constraint, Computational Experiments, Turning Angle, Bitangent
MSC2010: 90C57, 90C27, 90C11

1 Introduction

The *Traveling Salesman Problem* (TSP) is one of the best known and most widely investigated combinatorial optimization problems with several famous books entirely devoted to its study [4, 15, 18, 21]. Plenty of variations of this problem have already been studied (see e. g. [15]).

In this paper we consider a relevant extension of the TSP concerning its cost structure. While we are still looking for a Hamiltonian cycle, also called *tour*, we do not simply sum up the costs of the edges of the tour in the objective function, but we consider the transition in each vertex, i. e., for each vertex i we consider a cost or weight coefficient depending both on the predecessor and on the successor of i in the tour. Thus, we can model transition costs such as the effort of turning in path planning [2], changing the equipment in scheduling or the transportation means in logistic networks [3] from one edge to another.

Mathematically, this can be modeled via a quadratic objective function. The resulting optimization problem is known as *Symmetric Quadratic Traveling Salesman Problem* (SQTSP) [11]. Only a few publications have dealt with the SQTSP. Due to its quadratic cost structure, it is in general computationally much more difficult than the classical (linear) TSP.

1.1 Formal problem definition and related literature

In the SQTSP we associate costs with every pair of adjacent edges, represented by the corresponding triple of vertices. So, going from a vertex i to a vertex j using an edge (i, j) and then to a vertex k via edge (j, k) in a tour gives rise to a certain cost value which is assigned to the corresponding ordered triple denoted by $\langle i, j, k\rangle$. In this paper we consider the special case where the direction of traversal of the tour is irrelevant and so the costs for $\langle i, j, k\rangle$ and $\langle k, j, i\rangle$ are identical.

Our notation follows [11]. Let $V = \{1, 2, \ldots, n\}$ be a vertex set. An edge $e := (i, j) \in V^{\{2\}} := \big\{(i, j) = (j, i) \colon i, j \in V, i \neq j\big\}$ consists of an undirected pair of vertices and a 2-*edge* $e^{\langle 3\rangle} := \langle i, j, k\rangle \in V^{\langle 3\rangle} := \big\{\langle i, j, k\rangle = \langle k, j, i\rangle \colon i, j, k \in V, |\{i, j, k\}| = 3\big\}$ is defined as a sequence of three distinct vertices where the reverse sequence is regarded as identical. If there is no danger of confusion, we simply write ij instead of (i, j) and ijk instead of $\langle i, j, k\rangle$. Furthermore, we define a 2-*graph* $G = (V, A)$ as a pair of a vertex set V and a set of 2-edges $A \subseteq V^{\langle 3\rangle}$. A 2-graph is called *complete* if $A = V^{\langle 3\rangle}$. Finally, a *tour* $T = \big(\sigma(1), \sigma(2), \ldots, \sigma(n)\big)$ is a permutation σ of the vertices 1, 2, ..., n.

Given a complete 2-graph $G = (V, V^{\langle 3\rangle})$ with $n \geq 3$ and non-negative weights $d_{e^{\langle 3\rangle}} \in \mathbb{R}_0^+$ for every 2-edge $e^{\langle 3\rangle} \in V^{\langle 3\rangle}$, the SQTSP asks for a tour T with minimal total weight with respect to the 2-edge weights $d_{e^{\langle 3\rangle}}$, i. e., a tour T minimizing the objective function

$$f(G, T) := \left(\sum_{i=1}^{n-2} d_{\sigma(i)\sigma(i+1)\sigma(i+2)}\right) + d_{\sigma(n-1)\sigma(n)\sigma(1)} + d_{\sigma(n)\sigma(1)\sigma(2)}. \tag{1}$$

We will also consider the maximization version of that problem, which has not been studied in the literature before. Formally, the *Maximum Symmetric Quadratic Traveling Salesman Problem* (MaxSQTSP) asks for a tour T of *maximal* total weight w. r. t. (1).

The quadratic TSP was first introduced by Jäger and Molitor [17] in its more general asymmetric version with a motivation from biology, see also [12]. The authors provide seven different heuristics and two exact solution approaches for the asymmetric version. Polyhedral studies on the SQTSP were done by Fischer and Helmberg [11] who also derived several classes of strengthened subtour elimination constraints and proved that many of them are facet defining. They also provide computational comparisons based on an ILP linearization and on the standard separation approach known from the TSP literature (see e. g. [21]).

An important application of the SQTSP arises in robotics. Aggarwal et al. [2] discussed the situation of a robot where changing the driving directions is more energy consuming for larger turning angles. Thus, one would prefer a tour which keeps the movement of the robot as closely as possible to a straight line. Formally, the following *Angular-Metric Traveling Salesman Problem* (Angle TSP) was introduced in [2]. We assume in this case that the vertices correspond to points in the Euclidean plane and that the weights of the 2-edges d_{ijk} are given by the *turning angles* α_{ijk} (see Figure 1) defined as

$$d_{ijk} = \alpha_{ijk} := \arccos_{[0,\pi]} \left(\frac{j-i}{\|j-i\|} \cdot \frac{k-j}{\|k-j\|} \right) \tag{2}$$

where the dot $\cdot$ denotes the scalar product. In slight abuse of notation we will sometimes also use the notation $\langle i, j, i \rangle, i, j \in V, i \neq j$, for going from i to j and immediately back to i. Then (2) gives $\alpha_{iji} = \arccos(-1) = \pi$.

Combining in a weighted sum the turning angles with Euclidean distances of points in the plane gives rise to the *Angular-Distance Metric Traveling Salesman Problem* (Angle-Distance TSP). Problems of this kind were introduced in [22] for an approximate solution of the *TSP for Dubins vehicle*, which has applications in robotics.

Considering the SQTSP from an approximation point of view only few results are known. It is easy to see that the standard TSP with weights d'_{ij} can be represented as a special case of the SQTSP with identical solution value by defining 2-edge weights $d_{ijk} := d'_{jk}$ for all $ijk \in V^{\langle 3 \rangle}, i < k$. Thus, the well-known fact that no constant-ratio approximation can exist for the TSP immediately carries over to the SQTSP.

For the special case of the Angle TSP it was shown by Aggarwal et al. [2] that the problem is still $\mathcal{NP}$-hard but allows a polynomial time approximation algorithm guaranteeing an approximation ratio within $O(\log n)$.

For the complexity of the MaxSQTSP one can easily derive the following result.

Proposition 1. *MaxSQTSP is Max-$\mathcal{SNP}$-hard.*

Proof. It is known that the *Symmetric Maximum Traveling Salesman Problem* (MaxTSP) is Max-$\mathcal{SNP}$-hard [15, ch. 12]. Thus, the result follows from the above reduction. □

Proposition 1 implies that there exists a constant ratio approximation for the MaxSQTSP but the existence of a PTAS is highly unlikely.

In analogy to the Angle TSP we will also consider the *Maximum Angular-Metric Traveling Salesman Problem* (MaxAngle TSP) where the sum of the turning angles should be *large*, i. e., the sum of the angles contained between two adjacent edges should be as small as possible. Thus, we can consider the problem as a minimization problem where the weights $\widehat{d}_{ijk}$ are given by the *inner angles* as illustrated in Figure 1 and defined by

$$\widehat{d}_{ijk} = \widehat{\alpha}_{ijk} := \pi - \alpha_{ijk}. \tag{3}$$

The corresponding *reverse objective value* of a tour T is defined as

$$\widehat{f}(G,T) := n \cdot \pi - f(G,T). \tag{4}$$

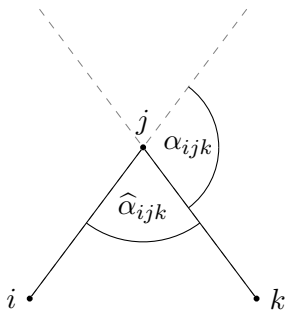

Figure 1: Illustration of the *turning angle* α_{ijk} and of the *inner angle* $\widehat{\alpha}_{ijk}$.

Our considerations of the MaxAngle TSP are related to [8, 9] where one studies angle-restricted tours. Given points in the Euclidean plane the authors investigate in which cases there exist tours such that all inner angles belong to some finite set and consider the complexity of the corresponding decision problems. Fekete and Woeginger [9] prove that there always exists a so called "pseudo-convex" tour if there are at least five vertices, i. e., a tour such that along the tour we always move clockwise (or always counterclockwise). Our result on the MaxAngle TSP for an odd number of vertices will imply the result in [9] in this case. Furthermore, in [8] it is shown that there always exists a tour such that the largest inner angle is at most $\frac{2\pi}{3}$ if the number of vertices is even.

1.2 Our contribution

The previous ILP-based solution approaches in [11, 12] all perform separation processes to identify the violated subtour elimination constraints on fractional solutions of a linearized model. On contrary, motivated by the impressive performance of today's ILP solvers we will pursue the strategy to do all separation processes only on integral solutions (see Section 2). This was tested with very limited success for the standard TSP in [20] but turned out to be much more promising for SQTSP. In Section 4 we will combine this approach with different variants of the classical subtour elimination constraints [6] and the strengthened variants introduced in [11]. We also give experimental results for the MaxSQTSP, which has never been treated in the literature before and turns out to be very challenging from a computational point of view. These computational studies are the first main contribution of this paper and show that in many cases our *integral approach* is faster in total and that sophisticated separation strategies do not pay off while solving the considered instances. The benchmark instances and the computational test environment of all our experiments are described in Section 3.

Second, we provide a completely different, mathematically interesting MILP linearization for the Angle TSP and Angle-Distance TSP in Section 4.2. This model has the advantage that only linearly many new variables are introduced. For instances of the Angle-Distance TSP with up to 55 vertices the running times can be improved. But for larger instances or classical Angle TSP instances our computational tests show that for larger n the branch-and-cut approaches based on the linearization in [11] are faster.

The third contribution concerns the theoretical solution structure of MaxAngle TSP. It is shown in Section 5.1 that there is a surprising split of the problem: For n odd, we show

that the reverse optimal solution value is always π, i. e., 180 degrees and the problem can be solved by the standard ILP model without producing any subtours. Nevertheless, even without subtour elimination constraints the solution of the remaining ILP, a 2-matching problem (also called *Cycle Cover Problem*), requires very large running times. Fortunately, we can bypass this difficulty since we can characterize the structure of an optimal solution and derive a simple constructive algorithm to find such an optimal solution. For n even, no such statement is possible and we can show that the reverse objective function is bounded by 0 from below and by 2π, i. e., 360 degrees from above. In particular we present a family of instances such that the optimal value of these converges to 2π for $n \to \infty$.

Finally, we conclude our work in Section 6.

2 Fractional vs. integral approach

The quadratic traveling salesman problem can be written as the following quadratic integer program with binary edge variables $x_e = x_{ij}$ for $e = (i,j) \in V^{\{2\}}$, with $\delta(i) := \{e\colon e = (i,j) \in V^{\{2\}}\}$ denoting the set of all edges incident with $i \in V$.

$$\min/\max \sum_{\substack{e^{\langle 3\rangle}=\langle i,j,k\rangle \in V^{\langle 3\rangle} \\ e=(i,j), f=(j,k)}} d_{e^{\langle 3\rangle}} x_e x_f \tag{5}$$

$$\text{s. t.} \sum_{e\in\delta(i)} x_e = 2, \qquad i \in V, \tag{6}$$

$$\sum_{\substack{e=(i,j)\in V^{\{2\}} \\ i,j\in S}} x_e \le |S| - 1, \qquad S \subsetneq V, S \neq \emptyset, \tag{7}$$

$$x_e \in \{0,1\}, \qquad e \in V^{\{2\}}. \tag{8}$$

In the objective function (5) a weight $d_{e^{\langle 3\rangle}}$ for some 2-edge $e^{\langle 3\rangle} \in V^{\langle 3\rangle}$ is taken into account if both edges $e = (i,j)$ and $f = (j,k)$ are contained in the tour. Equations (6) are the *degree constraints* ensuring that each vertex is visited once, (7) are the well-known *subtour elimination constraints* and, finally, (8) are the integrality constraints on the edge variables. In comparison to the standard model for the TSP going back to [6] we have only changed the objective function.

This quadratic integer program can easily be linearized by introducing a cubic number of additional binary variables $y_{e^{\langle 3\rangle}} = y_{ijk}$ for all 2-edges $e^{\langle 3\rangle} = \langle i,j,k\rangle \in V^{\langle 3\rangle}$, where $y_{ijk} = 1$ if and only if the vertices i, j and k are visited in the tour in consecutive order. This linearization was first introduced and extensively studied by Fischer and Helmberg [11].

$$\min/\max \sum_{e^{\langle 3\rangle}\in V^{\langle 3\rangle}} d_{e^{\langle 3\rangle}} y_{e^{\langle 3\rangle}} \tag{9}$$

$$\text{s. t. } (6), (7), (8),$$

$$x_e = \sum_{k\in V\setminus\{i,j\}} y_{ijk} = \sum_{k\in V\setminus\{i,j\}} y_{kij}, \qquad e = (i,j) \in V^{\{2\}}, \tag{10}$$

$$y_{e^{\langle 3\rangle}} \in \{0,1\}, \qquad e^{\langle 3\rangle} \in V^{\langle 3\rangle}. \tag{11}$$

The x-variables have to correspond to a tour. Apart from that this model has a linear objective function (9). Constraints (10) couple the x- and the y-variables. Finally, conditions (11) ensure the integrality of the y-variables.

This ILP can be used to solve the SQTSP by using the "standard" TSP techniques which were also applied in the computational studies in [11, 12]. In particular, we can separate the subtour elimination constraints (7) in the same way as described in the TSP literature (see e. g. [21]), i. e., by identifying the violated constraints on fractional solutions during the branch and cut solution process through the solution of appropriate min-cut problems.

In this paper we focus on a different strategy, which has already been tested for the classical TSP by Pferschy and Staněk [20]: We relax all subtour constraints (7) first and then solve the remaining model to integral optimality using an ILP solver. We get a 2-matching (a cycle cover) usually containing more than one cycle. These cycles can be found by a simple scan. Now, we can include a subtour elimination constraint for each such cycle and resolve the enlarged ILP model. This process is repeated and in each iteration additional subtour elimination constraints are added until we get a solution consisting of only one cycle, i. e., containing only an optimal SQTSP/MaxSQTSP tour. Note that in contrast to the TSP even the first step of the described procedure is an $\mathcal{NP}$-hard problem because the quadratic 2-matching problem is $\mathcal{NP}$-hard for the angular-metric case and for several variants [2, 12, 13].

A short pseudocode description of this approach is given in Algorithm 1. An example illustrating its execution is given in Figures 2–4: We can see that we need 3 iterations (ILP solver runs) and 4 (2 non-equivalent) subtour elimination constraints to solve the problem to optimality.

Require: SQTSP/MaxSQTSP instance
Ensure: an optimal SQTSP/MaxSQTSP tour
1: define current model as (6), (8), (9), (10), and (11);
2: **repeat**
3: solve the current model to optimality by an ILP-solver;
4: **if** solution contains no subtour **then**
5: **return** the solution as optimal tour;
6: **else**
7: find all subtours of the solution and add the corresponding subtour elimination constraints of type (7) to the current model;
8: **end if**
9: **until** optimal tour found;

Algorithm 1: Main idea of our elementary integral approach.

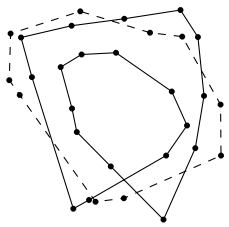

Figure 2: Angle-instance with $n = 30$: Iteration 1.

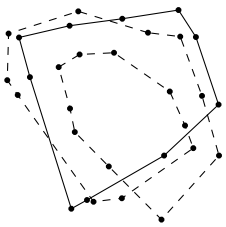

Figure 3: Angle-instance with $n = 30$: Iteration 2.

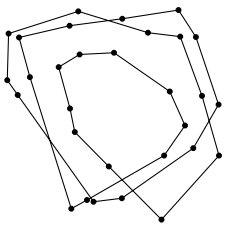

Figure 4: Angle-instance with $n = 30$: Optimal Angle TSP tour.

Let us concentrate on the subtour elimination constraints (7) first. They can be expressed

equivalently by the following cut constraints:

$$\sum_{\substack{e=(i,j)\in V^{\{2\}}\\ i\in S, j\in V\setminus S}} x_e \geq 2, \qquad S \subsetneq V, S \neq \emptyset. \tag{12}$$

Although mathematically equivalent, it has been observed that the two versions of forbidding a subtour may result in quite different performances of the ILP solver in the TSP context (see [20]). Thus we tested these two variants together with the combined variant

$$\begin{aligned} \sum_{\substack{e=(i,j)\in V^{\{2\}}\\ i,j\in S}} x_e &\leq |S|-1, \qquad \text{if } S \subset V, S \neq \emptyset, |S| \leq \frac{2n+1}{3}, \\ \sum_{\substack{e=(i,j)\in V^{\{2\}}\\ i\in S, j\in V\setminus S}} x_e &\geq 2, \qquad \text{if } S \subsetneq V, |S| > \frac{2n+1}{3}. \end{aligned} \tag{13}$$

So we choose the variant which adds less non-zero entries to the overall constraint matrix (see also Section 1 in [7] for some comments on constraints with large support). The computational results are summarized in Table 1 in the Appendix (see Section 3 for a detailed description of the benchmark instances and of the test environment). Our tests show that the combined variant (13) tends to slightly outperform the other two variants for randomly generated instances and for Angle-Distance TSP instances for larger n. Since this representation of subtour elimination constraints was also used in [20], we stick to using (13) for the basic reference methods F and I, i. e., for the *elementary fractional* and *elementary integral approach*, respectively, in the rest of this paper.

3 Computational experiments

In this section we describe the test setup of our computational experiments, which constitute a major part of this paper.

3.1 Benchmark instances

Our benchmark instances are mainly based on the instance specification developed in [10] and [11]. However, we usually do not round the costs to integers because the second MILP linearization to be introduced in Section 4.2 requires the exact turning angle values α for instances of the Angle TSP and the Angle-Distance TSP. We test three instance classes[1]:

Angle-instances are based on points in the Euclidean plane: First, we choose n points discrete uniformly at random out of $\{0,\ldots,500\}^2$ and then compute the *turning angles* α which we multiply by 1000 first and then we round them to 12 decimal places. The multiplicative constant of 1000 is introduced to allow a comparison of our programs with [10]. Instances of this type are named *Angle_n* where n denotes the number of points/vertices.

Angle-Distance-instances extend the above Angle-instances by combining them with the Euclidean distances between the points in a weighted sum. Taking the identical point sets in the plane as generated for *Angle_n* (to allow a better comparison) we denote

[1] All instances and optimal solution values can be downloaded from `http://optimierung.math.uni-goettingen.de/content/members/afischer/SQTSP.zip`.

the Euclidean distances between vertices i and j as d_{ij}. For a parameter $\rho \in \mathbb{R}_0^+$ we construct SQTSP-weights as follows:

$$d_{ijk} := 100 \left(\rho \cdot \alpha_{ijk} + \frac{d_{ij} + d_{jk}}{2} \right). \tag{14}$$

We again round all weights to 12 decimal places.

These instances are between Angle-instances (for $\rho \to \infty$) and standard TSP instances (for $\rho = 0$). For compatibility with the literature we set $\rho = 40$ for all our tests as done in [10]. Instances of this type are named *Angle-Distance_n*.

Random-instances assign random costs to all 2-edge weights d, in particular the costs are chosen discrete uniformly at random from $\{0, \ldots, 10000\}$. The resulting instances are named *Random_n*.

For each type of instance and each size n we generated 10 test instances.

3.2 Layout of test results

The tables in the Appendix are all created in the following way: The first column always contains the instance type and size. The second column contains the running times for the first method, which acts as a reference method in the particular table. All further columns report the ratios between the running times of the particular approaches and the reference method. The only exception concerns the *root node ratios* in Table 2 where the ratios between the values of the LP-relaxation in the root node and the optimal solution values are reported. We generated 10 instances for every instance type and every size n and report the mean values over these 10 instances, in particular *arithmetic means* for running times and *geometric means* for all ratios. Entries for instances where a particular method cannot be used are marked by "–" and, finally, entries for which we expected excessive running times were omitted from the tests and are marked by "Ø".

3.3 Test environment

All tests were run on an *Intel(R) Core(TM) i5-3470 CPU @ 3.20GHz with 16 GB RAM* under *Linux*[2] and all programs were implemented in *C++*[3] using *CPLEX* 12.6.1.0 as the ILP-solver. Moreover, in order to guarantee the relative reproducibility of our computational results, we (i) did not allow additional swap memory and (ii) ran all tests separately without other user processes in background.

4 Minimization problem

The minimization problem SQTSP and its special case Angle TSP were extensively studied by Fischer and Helmberg [11] from a theoretical point of view: After introducing the ILP linearization (6)–(11), stronger forms of subtour elimination constraints, which also involve the y-variables, were described and analyzed. Their paper also contains a small computational study which is based on a larger set of computational experiments reported in [10]. However, the authors only deal with the "standard" fractional approach and its variants.

[2]Precise version: *Linux 3.5.0-23-generic #35~precise1-Ubuntu SMP x86_64 x86_64 x86_64 GNU/Linux.*
[3]Precise compiler version: *gcc version 4.8.1.*

One main goal of this paper is to provide a broad computational comparison of different solution strategies. First, we compare the elementary fractional approach with the elementary integral approach and then we combine both approaches with the stronger subtour elimination constraints from [11] in Section 4.1. In this section we also examine some weaker types of subtour elimination constraints. Finally, in Section 4.2 we introduce a new and completely different MILP linearization with only a linear number of additional variables. It is based on a geometric argument and works only for Angle- and Angle-Distance-instances.

Our first computational results are given in Table 2 of the Appendix. The first column (F) contains the results for the *elementary fractional* and the third column (I) the results for the *elementary integral approach*. We can see that the elementary integral approach outperforms the elementary fractional approach significantly and, moreover, this trend seems to increase for larger n for all classes of test instances. This behavior is quite surprising since the analogous integral solution strategies are clearly outperformed by the fractional ones for the standard TSP as illustrated in [20]. To find an explanation for this difference we analyzed numerous test instances individually and could observe one main difference between SQTSP and TSP: The SQTSP instances usually produce significantly less subtour elimination constraints than the TSP instances of similar size and thus solving them involves much less ILP solver runs. In fact, we obtained less than 10 subtour elimination constraints for most of our test instances. By studying the particular stages of the solution process for the Angle- and Angle-Distance-instances we could also observe that the structure of the generated subtours is different: While the subtours in the TSP case are typically small and often consist of only a few vertices (and thus we might have many of them), for the SQTSP instances we obtained large subtours. For the Angle TSP the subtours have the form of large "circles" or "spiral" shapes. This behavior was also illustrated in the example of Figures 2, 3 and 4, where only four (two non-equivalent) subtour elimination constraints were required for determining an optimal SQTSP tour.

4.1 Extending the subtour elimination constraints

In this section, we extend the elementary fractional and the elementary integral approach by including the subtour elimination constraints introduced in [11]. We also examine some variants of these constraints. More detailed descriptions and illustrations of the underlying geometric ideas can be found in [10]. All computational results for the introduced variants are summarized in Tables 3 and 4 in the Appendix.

F(I)/I(I): We try to reduce the number of unnecessary subtour elimination constraints in this variant. In fact, one subtour elimination constraint can be skipped in every iteration as the corresponding tour is implicitly excluded by the other ones. Thus we always omit the constraint for the largest subtour (i. e., for the subtour which causes the most non-zero entries in the constraint matrix).

Since we introduce in every iteration only one subtour elimination constraint less than in the *elementary fractional* / *elementary integral* approach, we cannot expect huge computational time improvements. Indeed, the methods F(I)/I(I) perform similarly to F/I for the Angle- and Angle-Distance-instances. We can observe a larger variance of the ratios for the Random-instances, but this trend does not seem to hold for larger values of n.

F(II)/I(II): In this variant, we weaken the constraints (7) by including the x-variables only for pairs of vertices i, j that are connected with an edge in the particular subtour.

So we have

$$\sum_{\substack{e=(i,j)\in V^{\{2\}}\\ i,j\in S\\ x^*_{ij}=1}} x_e \le |S|-1, \qquad S\subsetneq V, S\neq\emptyset, \tag{15}$$

where $x^*_{ij}=1$ if the vertices i and j are connected by an edge in the current solution. Since there does not exist a cut version of such a subtour elimination constraint, we always use (15) independently of the subtour size $|S|$.

Also this variant performs mostly similarly to our *elementary approaches*. This is a bit surprising because this kind of subtour elimination constraints is significantly weaker from a theoretical point of view if $|S|>3$.

F(III)/I(III): We use the strengthened variant of the subtour elimination constraints introduced in [11]. They are based on the idea that a y-variable y_{ikj}, $ikj\in V^{\langle 3\rangle}$, almost acts like an x-variable x_{ij}, $ij\in V^{\{2\}}$. If they are one in a solution both express that the nodes i and j are close in the tour. So, in the following formulas we do not only count the number of direct connections between the nodes of some set S, but also the connections that leave S but immediately return. We get

$$\begin{aligned}
&\sum_{\substack{e=(i,j)\in V^{\{2\}}\\ i,j\in S}} x_e + \sum_{\substack{e^{\langle 3\rangle}=\langle i,k,j\rangle\in V^{\langle 3\rangle}\\ i,j\in S,k\in V\setminus S}} y_{e^{\langle 3\rangle}} \le |S|-1, && S\subset V, S\neq\emptyset, |S|<\frac{n}{2},\\
&\sum_{\substack{e=(i,j)\in V^{\{2\}}\\ i,j\in S}} x_e + \sum_{\substack{e^{\langle 3\rangle}=\langle i,k,j\rangle\in V^{\langle 3\rangle}\\ i,j\in S,k\in V\setminus (S\cup\{\widehat{t}\})}} y_{e^{\langle 3\rangle}} \le |S|-1, && S\subsetneq V, |S|\ge\frac{n}{2}, \widehat{t}\in V\setminus S,
\end{aligned} \tag{16}$$

as a stronger form of (7) and, similarly,

$$\begin{aligned}
&\sum_{\substack{e=(i,j)\in V^{\{2\}}\\ i\in S,j\in V\setminus S}} x_e - 2\sum_{\substack{e^{\langle 3\rangle}=\langle i,k,j\rangle\in V^{\langle 3\rangle}\\ i,j\in S,k\in V\setminus S}} y_{e^{\langle 3\rangle}} \ge 2, && S\subset V, S\neq\emptyset, |S|<\frac{n}{2},\\
&\sum_{\substack{e=(i,j)\in V^{\{2\}}\\ i\in S,j\in V\setminus S}} x_e - 2\sum_{\substack{e^{\langle 3\rangle}=\langle i,k,j\rangle\in V^{\langle 3\rangle}\\ i,j\in S,k\in V\setminus (S\cup\{\widehat{t}\})}} y_{e^{\langle 3\rangle}} \ge 2, && S\subsetneq V, |S|\ge\frac{n}{2}, \widehat{t}\in V\setminus S,
\end{aligned} \tag{17}$$

as a stronger form of the cut variant (12), which is equivalent to (16). These can be interpreted in the following way. We only count those edges leaving S that do not immediately reenter S. Note, if $|S|\ge\frac{n}{2}$ then we have to exclude one vertex $\widehat{t}\in V\setminus S$ in the summation to avoid forbidding tours in both variants (for detailed proofs see [11]). The inequalities are valid for arbitrary choices of $\widehat{t}\in V\setminus S$. In our test we add only one inequality using

$$\widehat{t}=\operatorname*{arg\,max}_{k\in V\setminus S}\left\{\min_{\substack{i,j\in S\\ i\neq j}} d_{ikj}\right\}, \tag{18}$$

although the influence of this choice seems to be rather limited. Finally, we keep the case distinction introduced in (13) and thus use (16) if $|S|\le\frac{2n+1}{3}$ and (17) otherwise.

Although these strengthened subtour elimination constraints are facet defining for the SQTSP polytope as long as $2\le|S|\le n-3$ and the constraints are much stronger than (7) from a theoretical point of view, we cannot observe any computational time improvements in Tables 3 and 4. On the contrary, these kinds of subtour elimination

constraints increase the computational times for almost all test instance groups and this trend becomes even stronger for larger values of n. Additionally, we want to note that determining a maximally violated inequality (16) in the case $|S| < \frac{n}{2}$ is an $\mathcal{NP}$-hard problem [11], the complexity of the separation problem is currently unknown.

F(IV)/I(IV): This variant combines the subtour elimination constraints used in F(III) and I(III) with the idea introduced for F(II) and I(II), however, this idea is adopted only for the y-variables. So we add the associated y-variable to the left-hand side of a constraint if and only if $x^*_{ij} = 1$ in (16) or (17) in the current solution, where $x^*_{ij} = 1$ if the vertices i and j are connected by an edge in the current solution. In particular, we get

$$\begin{aligned}
&\sum_{\substack{e=(i,j)\in V^{\{2\}}\\ i,j\in S}} x_e + \sum_{\substack{e^{\langle 3\rangle}=\langle i,k,j\rangle\in V^{\langle 3\rangle}\\ i,j\in S, k\in V\setminus S\\ x^*_{ij}=1}} y_{e^{\langle 3\rangle}} \le |S|-1, && S\subset V, S\neq\emptyset, |S|<\frac{n}{2},\\
&\sum_{\substack{e=(i,j)\in V^{\{2\}}\\ i,j\in S}} x_e + \sum_{\substack{e^{\langle 3\rangle}=\langle i,k,j\rangle\in V^{\langle 3\rangle}\\ i,j\in S, k\in V\setminus(S\cup\{\widehat{t}\})\\ x^*_{ij}=1}} y_{e^{\langle 3\rangle}} \le |S|-1, && S\subsetneq V, |S|\ge\frac{n}{2}, \widehat{t}\in V\setminus S,
\end{aligned} \tag{19}$$

as a variant of (16). Subsequently, the cut variant (17) can be adapted in the same way.

This idea tries to reduce the number of non-zero entries in the constraint matrix and can be seen as the compromise between the *elementary approaches* and variants (III). Obviously, we lose the facetness of the added inequalities.

Looking at the running times, we can expect that these fluctuate between F/I and F(III)/I(III) as well. Indeed, in our tests the results for the methods F(IV)/I(IV) are slightly worse than the results for F/I and a bit better than the results for F(III)/I(III).

F(V)/I(V): We use an equivalent version of (16) or (17), respectively, that only uses y-variables,

$$\begin{aligned}
&\sum_{\substack{e^{\langle 3\rangle}=\langle i,j,k\rangle\in V^{\langle 3\rangle}\\ i\in S, j,k\in V\setminus S}} y_{e^{\langle 3\rangle}} \ge 2, && S\subset V, S\neq\emptyset, |S|<\frac{n}{2},\\
&\sum_{\substack{e^{\langle 3\rangle}=\langle i,j,k\rangle\in V^{\langle 3\rangle}\\ i\in S, j,k\in V\setminus S}} y_{e^{\langle 3\rangle}} + 2\sum_{\substack{e^{\langle 3\rangle}=\langle i,\widehat{t},j\rangle\in V^{\langle 3\rangle}\\ i,j\in S}} y_{e^{\langle 3\rangle}} \ge 2, && S\subsetneq V, |S|\ge\frac{n}{2}, \widehat{t}\in V\setminus S,
\end{aligned} \tag{20}$$

where we restrict to $\widehat{t}$ as in (18) in our tests. They can be interpreted similarly to the constraints above. We only count those 2-edges that leave the set S without immediately returning. In our tests, we always use (20) independently of the subtour size $|S|$.

These constraints are facet defining if $n \ge 6$ and $2 \le |S| \le n-3$ (see [11]), but do not speed up the solution process, as can be seen in Tables 3 and 4: The methods F(V)/I(V) tend to perform worse for all instance groups (at least for larger n) and they are significantly worse for the Angle-instances.

Finally, let us summarize the computational results in Tables 3 and 4. We can observe that subtour elimination constraints, which are stronger from a theoretical point of view, tend to slow down the algorithm. This fact is surprising since one would expect that

stronger models will lead to better bounds during the solution process. One possible explanation might be the number of non-zero entries in the constraint matrix (see [7]): The methods F(I)/I(I) and F(II)/I(II) perform similarly to the *elementary approaches* F/I, whereas variants F(III)/I(III), F(IV)/I(IV) and F(V)/I(V) all require larger running times and all have a larger number of non-zero entries in their constraint matrix. However, since we use the ILP solver as a "black box", this is only a guess.

4.2 A geometry-based MILP linearization for Angle TSP

The standard linearization described in Section 2 requires a *cubic* number of additional integer variables $y_{e^{\langle 3\rangle}}, e^{\langle 3\rangle} \in V^{\langle 3\rangle}$. Exploiting the geometry of the Angle TSP we can derive a different linearization adding only a *linear* number of real-valued variables. A related construction was used in [19] for a single allocation hub location problem. Clearly, this approach can be applied immediately also for the Angle-Distance TSP by splitting the objective function into a linear distance component and the turning angle:

$$\min w_1 \sum_{e \in V^{\{2\}}} d_e x_e + w_2 \sum_{\substack{e^{\langle 3\rangle}=\langle i,j,k\rangle \in V^{\langle 3\rangle} \\ e=(i,j), f=(j,k)}} \alpha_{e^{\langle 3\rangle}} x_e x_f. \tag{21}$$

Euclidean distances between vertices i and j are denoted by $d_e = d_{ij}$ and $\alpha_{e^{\langle 3\rangle}} = \alpha_{ijk}$ gives the *turning angle* as defined in (2). The parameters w_1 and w_2 can be used to weight the two components of the objective function. Our Angle-instances and Angle-Distance-instances defined in Section 3.1 correspond to the settings $w_1 = 0$, $w_2 = 1000$ and $w_1 = 100$, $w_2 = 4000$, respectively.

The quadratic terms in the second part of (21) can be easily moved into the set of constraints by introducing a new variable $y_j \in \mathbb{R}_0^+$ for every vertex $j \in V$ corresponding to the turning angle of a tour in vertex j. Thus, we replace (21) by

$$\min w_1 \sum_{e \in V^{\{2\}}} d_e x_e + w_2 \sum_{j \in V} y_j \tag{22}$$

with

$$y_j \geq \sum_{\substack{i,k \in V \setminus \{j\} \\ i<k}} \alpha_{ijk} x_{ij} x_{jk}, \qquad j \in V, \tag{23}$$

as new constraints. We will now prove that the set of quadratic inequalities of type (23) is – assuming that the degree constraints (6) and the integrality conditions (8) are satisfied – equivalent to the following linear inequalities:

$$y_j \geq \sum_{k \in V \setminus \{j\}} \alpha_{ijk} x_{jk} - \pi, \qquad i, j \in V, i \neq j. \tag{24}$$

For the proof we need the following geometric lemma.

Lemma 2. *For each $i, j, k, l \in V$ with $i \neq j$, $k \neq j$ and $l \neq j$ we have*

$$\alpha_{ijk} + \pi \geq \alpha_{ljk} + \alpha_{lji}. \tag{25}$$

Proof. Recall from (3) that $\widehat{\alpha}_{ijk} = \pi - \alpha_{ijk}$ denotes the *inner angle*. For any $l \in V$ we have $\widehat{\alpha}_{ijl} + \widehat{\alpha}_{ljk} \geq \widehat{\alpha}_{ijk}$ which shows the claim (using also the symmetry of the first and last index in $\widehat{\alpha}$). □

Theorem 3. *The set of constraints* (6) *and* (23) *is equivalent to the set of constraints* (6) *and* (24) *for binary variables* $x_{ij} \in \{0,1\}$, $ij \in V^{\{2\}}$, *and variables* $y_j \in \mathbb{R}_0^+$, $j \in V$.

Proof. Assume first that (6) and (23) are satisfied. Let $j \in V$ be fixed. Then we can do the following calculation by applying Lemma 2 for a vertex $l \in V, l \neq j$:

$$\begin{aligned}
y_j &\geq \sum_{\substack{i,k \in V\setminus\{j\} \\ i<k}} \alpha_{ijk} x_{ij} x_{jk} \;\geq \sum_{\substack{i,k \in V\setminus\{j\} \\ i<k}} \big(\alpha_{ljk} + \alpha_{lji} - \pi\big) x_{ij} x_{jk} \\
&= \sum_{\substack{i,k \in V\setminus\{j\} \\ i<k}} \alpha_{ljk} x_{ij} x_{jk} + \sum_{\substack{i,k \in V\setminus\{j\} \\ i<k}} \alpha_{lji} x_{ij} x_{jk} - \pi \sum_{\substack{i,k \in V\setminus\{j\} \\ i<k}} x_{ij} x_{jk} \\
&\overset{i \leftrightarrows k}{=} \sum_{\substack{i,k \in V\setminus\{j\} \\ i<k}} \alpha_{ljk} x_{ij} x_{jk} + \sum_{\substack{i,k \in V\setminus\{j\} \\ k<i}} \alpha_{ljk} x_{kj} x_{ji} - \pi \sum_{\substack{i,k \in V\setminus\{j\} \\ i<k}} x_{ij} x_{jk} \\
&= \sum_{\substack{i,k \in V\setminus\{j\} \\ i\neq k}} \alpha_{ljk} x_{ij} x_{jk} \; - \tfrac{\pi}{2} \sum_{\substack{i,k \in V\setminus\{j\} \\ i\neq k}} x_{ij} x_{jk}.
\end{aligned}$$

Then we eliminate the condition $i \neq k$ by subtracting the sum for $i = k$ and exploit the binarity of the x-variables. This results in:

$$\begin{aligned}
y_j &\geq \sum_{i,k \in V\setminus\{j\}} \alpha_{ljk} x_{ij} x_{jk} \; - \sum_{k \in V\setminus\{j\}} \alpha_{ljk} x_{kj} x_{kj} - \tfrac{\pi}{2} \left(\sum_{i,k \in V\setminus\{j\}} x_{ij} x_{jk} - \sum_{k \in V\setminus\{j\}} x_{jk} x_{jk} \right) \\
&= \sum_{k \in V\setminus\{j\}} \alpha_{ljk} x_{jk} \sum_{i \in V\setminus\{j\}} x_{ij} - \sum_{k \in V\setminus\{j\}} \alpha_{ljk} x_{kj} - \tfrac{\pi}{2} \left(\sum_{i \in V\setminus\{j\}} x_{ij} \sum_{k \in V\setminus\{j\}} x_{jk} - \sum_{k \in V\setminus\{j\}} x_{jk} \right) \\
&\overset{(6)}{=} \sum_{k \in V\setminus\{j\}} \alpha_{ljk} x_{jk} \cdot 2 - \sum_{k \in V\setminus\{j\}} \alpha_{ljk} x_{kj} - \pi \;=\; \sum_{k \in V\setminus\{j\}} \alpha_{ljk} x_{jk} - \pi.
\end{aligned}$$

This shows that (6) and (23) together with the integrality of the x-variables imply (24).

To prove the other direction, let us assume that $\widehat{x}, \widehat{y}$ satisfy (6) and (24). For every $j \in V$, (6) implies the existence of i_j and k_j with $\widehat{x}_{i_j j} = 1$, $\widehat{x}_{k_j j} = 1$ and $\widehat{x}_{ij} = 0$ for all $i \in V, i \notin \{i_j, k_j\}$. Now we evaluate (24) for $i = i_j$:

$$\widehat{y}_j \geq \sum_{k \in V\setminus\{j\}} \alpha_{i_j j k} \, \widehat{x}_{jk} - \pi = \alpha_{i_j j k_j} + \alpha_{i_j j i_j} - \pi = \alpha_{i_j j k_j} = \sum_{\substack{i,k \in V\setminus\{j\} \\ i<k}} \alpha_{ijk} \, \widehat{x}_{ij} \widehat{x}_{jk}.$$

Therefore, $\widehat{x}, \widehat{y}$ also satisfy (23). □

Computational experiments for the linearization given by (24) are reported in Table 2 in the Appendix. Two variants were tested, the former using the standard separation process done on fractional solutions (column $\mathrm{F^L}$) and the latter based on the integer subtour approach (column $\mathrm{I^L}$). It turns out that the linearization works quite well for medium-sized Angle-Distance-instances with up to 55 vertices where it is superior to the respective elementary versions. However, for larger n it is clearly outperformed by the *elementary fractional* and by the *elementary integral approach*. Moreover, the performance is significantly worse for all Angle-instances. Recall that this approach can be used neither for the Random-instances nor for the maximization problems.

From a theoretical perspective it is also interesting to look at the root node gap, i. e., the difference between values of the LP-relaxation in the root node of the ILP-solver (without

any subtour constraints) for both linearizations and the optimal solution values. Clearly, these are the same for the fractional and integral approaches since the differences in the subtour elimination have effects only later. In Table 2 we report the corresponding ratios in columns *ratio* and $ratio^{\mathrm{L}}$. It can be seen that the linearization with (24) yields larger root node gaps for all instance classes. Yet they do not differ for the Angle-Distance-instances as much as for the Angle-instances, which may explain the differences in performance. However, it should also be pointed out that in the Angle-Distance-instances the linearization of the y-variables is less significant than for the Angle-instances due to the weighted sum in the objective function given by the parameters w_1 and w_2. It can be assumed that the behavior of both linearizations would converge for both models as $\rho \to 0$, i. e., $w_2 \to 0$ in (22).

The close relationship to the TSP may also be the reason for the extremely small variance between the root node ratios for different Angle-Distance-instances. Beardwood et al. [5] proved that the expected length of an optimal TSP tour is asymptotically equal to $\beta\sqrt{n}$, where β is a constant, if uniformly random points in the Euclidean planes are considered. Moreover, Pferschy and Staněk [20] empirically observed that this convergence property leads to very small variances of TSP solution values even for small values of n. A similar behavior can be observed in Table 2 where the average root node ratios for the Angle-Distance-instances do not vary at all.

Summarizing, this linearization does not yield competitive results for large instances with at least 60 vertices and thus we did not consider it with the other variants of subtour elimination constraints given in Section 4.1.

5 Maximization problem

In this section we deal with the maximization variant of the SQTSP. First, we focus on the MaxAngle TSP from a theoretical point of view and then we provide computational tests for all instance classes of the MaxSQTSP as in the minimization case.

5.1 Theoretical Analysis of MaxAngle TSP

Recall that for the MaxAngle TSP the vertices of the graph correspond to points in the Euclidean plane and the weights d_{ijk} represent the turning angles α_{ijk} for all $i, j, k \in V, i \neq j, k \neq j$. Moreover, in (3) and (4) we defined inner angles $\widehat{\alpha}_{ijk} := \pi - \alpha_{ijk}$ and the corresponding reverse objective value $\widehat{f}(G,T) := n \cdot \pi - f(G,T)$ for a tour T. It will be convenient to address MaxAngle TSP as a *minimization* problem w. r. t. $\widehat{f}(G,T)$.

While for SQTSP there is not a fundamental difference between Angle-instances and other instance groups, there is a surprising and highly interesting dichotomous behavior to be observed for MaxAngle TSP. We will show below that the optimal reverse objective value equals π for any instance if n is odd. This means that for odd n the optimal solution value of MaxAngle TSP does not require any computation at all. Note that this remarkable result implies that the solution of MaxAngle TSP by our integral approach will never produce any subtour elimination constraint if the vertices are in non-collinear position and so we need exactly one iteration step without adding subtour elimination constraints at all. This follows from the observation that any partition of the odd vertex set into subtours will contain at least one subset of odd cardinality which again would have an optimal reverse objective value equal to π on its own. As every subset of even cardinality implies a solution having a positive reverse objective value (at least for non-collinear vertices), the overall reverse objective value of such a solution is strictly greater than π and thus this solution cannot be optimal. Nevertheless, even without subtours the solution of the ILP model for odd instances of MaxAngle TSP by a standard solver requires extensive running times as

described in Section 5.2. As an alternative solution variant we will present a constructive algorithm, which calculates an optimal tour in polynomial time.

For n even there does not hold an equivalent statement. In fact, the optimal value of the reverse objective function can attain values between 0 and 2π in this case and these bounds are tight.

5.1.1 MaxAngle TSP: n is odd

Let n be odd. First, we prove that $\widehat{f}(G,T) \geq \pi$ for every tour T and thereafter we provide a constructive algorithm which yields a tour T^* reaching this lower bound, i. e., with $\widehat{f}(G,T^*) = \pi$.

Let ijk be three vertices traversed in succession in a tour T. If the vertex k lies left to the ray $\overrightarrow{ij}$, we say that the tour T has a *counterclockwise turn* in the vertex j. Otherwise, we say that the tour T has a *clockwise turn* in the vertex $j \in V$ (if the vertex k lies on the line ij, we say that the tour has a clockwise turn in the vertex j as well).

Lemma 4. *Let $G = (V, A)$ be an instance of MaxAngle TSP. If n is odd, then the following holds for any tour T:*

$$\widehat{f}(G,T) \geq \pi. \tag{26}$$

Proof. Consider an arbitrary tour T in G and let $\overline{C} \subseteq V$ be the set of vertices in which the tour T has a counterclockwise turn and $C \subseteq V$ the set of vertices in which the tour T has a clockwise turn. Furthermore, let us define the turning angles of T in j as $\alpha_j^T := \alpha_{ijk}$ and $\widehat{\alpha}_j^T := \widehat{\alpha}_{ijk}$, where ijk are three vertices traversed in succession in the tour T. Since the tour T has to be closed, there is

$$\sum_{j\in\overline{C}} \alpha_j^T - \sum_{j\in C} \alpha_j^T = 2\pi k$$

for some $k \in \mathbb{Z}$. This identity can be reformulated by using (3):

$$\begin{aligned}
\sum_{j\in\overline{C}} (\pi - \widehat{\alpha}_j^T) - \sum_{j\in C} (\pi - \widehat{\alpha}_j^T) &= 2\pi k \\
\big(|\overline{C}| \cdot \pi - \sum_{j\in\overline{C}} \widehat{\alpha}_j^T\big) - \big(|C| \cdot \pi - \sum_{j\in C} \widehat{\alpha}_j^T\big) &= 2\pi k \\
\big(|\overline{C}| - |C|\big)\pi - \sum_{j\in\overline{C}} \widehat{\alpha}_j^T + \sum_{j\in C} \widehat{\alpha}_j^T &= 2\pi k.
\end{aligned}$$

Since either $|\overline{C}|$ or $|C|$ is odd we get

$$\sum_{j\in C} \widehat{\alpha}_j^T - \sum_{j\in\overline{C}} \widehat{\alpha}_j^T = \pi + 2\pi k'$$

for some $k' \in \mathbb{Z}$. Moreover,

$$\sum_{j\in V} \widehat{\alpha}_j^T = \sum_{j\in C} \widehat{\alpha}_j^T + \sum_{j\in\overline{C}} \widehat{\alpha}_j^T \geq \big|\sum_{j\in C} \widehat{\alpha}_j^T - \sum_{j\in\overline{C}} \widehat{\alpha}_j^T\big| = |\pi + 2\pi k'|$$

and thus

$$\widehat{f}(G,T) \geq \pi. \qquad \square$$

Observe that the proof also reveals an interesting property of the structure of T in case $\widehat{f}(G,T) = \pi$. This extremal situation can only happen if $\sum_{j\in C} \widehat{\alpha}_j^T + \sum_{j\in\overline{C}} \widehat{\alpha}_j^T$ equals $\big|\sum_{j\in C} \widehat{\alpha}_j^T - \sum_{j\in\overline{C}} \widehat{\alpha}_j^T\big|$, which is only the case if all turns of the tour have the same orientation.

In the following we show by a constructive argument that the lower bound of Lemma 4 can always be reached.

Theorem 5. *For n being odd there exists a solution to the MaxAngle TSP with reverse objective value π. This tour can be constructed in $O(n \log n)$ time.*

Proof. Let P be a set of n points in the Euclidean plane in general position, i. e., no three points are on a line. Let $p \in P$ be an extreme point of P, i. e., a vertex of the convex hull $\mathrm{CH}(P)$ of P, and let v be a line through p that separates $P \setminus \{p\}$ into two equal halves. For ease of presentation, we rotate the plane such that v becomes vertical, in a way that the bottommost point of v inside the convex hull of P be p. Let $L \subset P$ be the points to the left of v and $R \subset P$ be the points to the right of it. We have $|L| = |R| = \frac{n-1}{2}$. Let b be a line that (i) contains a point $l \in L$ and a point $r \in R$, that (ii) is directed from r to l, and that (iii) has $\mathrm{CH}(L)$ in its left closed half-plane and $\mathrm{CH}(R)$ in its right closed half-plane. See Figure 5 for an illustration. We call b the *counterclockwise bitangent* of L and R. Note that p is to the left of b. We set $l_1 := l$ and let l_1 be the successor of p in our tour. Next, we consider the counterclockwise bitangent of $L \setminus \{l_1\}$ and R, which is defined by two points $r' \in R$ and $l' \in L \setminus \{l_1\}$. Note that r' may be different from r. We set $r_1 := r'$ and let r_1 be the successor of l_1 in our tour. In general, we connect l_i to the point r_i that is on the counterclockwise bitangent of $L_i := L \setminus \{l_1, \ldots, l_i\}$ and $R_{i-1} := R \setminus \{r_1, \ldots, r_{i-1}\}$, and connect r_i to the point l_{i+1} that is on the counterclockwise bitangent of L_i and R_i. Finally, we connect the point $l_{(n-1)/2}$ to the unique remaining point $r_{(n-1)/2} \in R_{(n-1)/2-1}$ and, subsequently, we connect the point $r_{(n-1)/2}$ to p to close the tour.

We show that the tour makes a clockwise turn at r_i. Observe that l_i is to the right of the counterclockwise bitangent β of L_i and R_{i-1}, as it has been on the counterclockwise bitangent of L_{i-1} and R_{i-1} together with some point $r \in R$ (see Figure 6). By definition, r_i is on β, and it is also by definition that r_i is to the right of v. Thus v and β divide the plane into four quadrants, where l_i is on the upper-left quadrant, r_i is on β between the lower-right and the upper-right quadrant, and l_{i+1} can only be in the lower-left quadrant or on β between the upper-left and the lower-left quadrant. Hence, the tour makes a clockwise turn at r_i. Note that this also holds when L is empty and we connect $l_{(n-1)/2}$ to $r_{(n-1)/2}$ and $r_{(n-1)/2}$ to p. With the analogous arguments, we see that we always make a clockwise turn at each point in L. Observe that the slope of $l_i r_i$ is less than the slope of β (r_i is on β and l_i is in the upper-right quadrant), while the slope of $r_i l_{i+1}$ is equal to or greater than the slope of β.

Thus, our edges always intersect v, and their slopes are increasing. We can think of an upward-directed copy v' of v that rotates counterclockwise around p until it contains l_1, at which time it continues rotating around l_1 until it contains r_1 and so on. The slope of v' is increasing until it reaches p again, where we can rotate it counterclockwise around p until it matches v again. Therefore, v' is in total rotated by π, which is thus our reverse objective value. For an illustration of an optimal tour we refer to Figure 7.

Finally, observe that our argument also holds if there are three points on a line. In fact, if we are to choose the next point of, say, L and there are two points of L on the current counterclockwise bitangent, then we can choose either of them. The next counterclockwise bitangent will be identical to the current one, and we will end up with an angle of 0. Also, if our halving line v has to contain additional points, we can slightly perturb it to a halving line of $P \setminus \{p\}$ that does not contain any point by a counterclockwise rotation.

It remains to show that our construction can be done in $O(n \log n)$ time. Hershberger and Suri [16] give an $O(n \log n)$ time algorithm to construct a data structure that maintains the convex hull while deleting a sequence of up to n points. The overall cost of deleting these points is $O(n \log n)$. We apply this independently to our sets L and R. Since

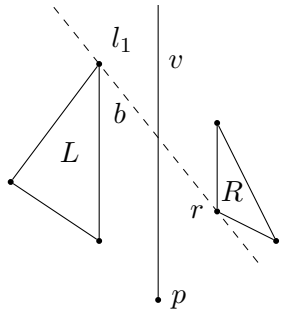

Figure 5: Angle-instance with $n = 7$: Construction of an optimal tour: phase 1.

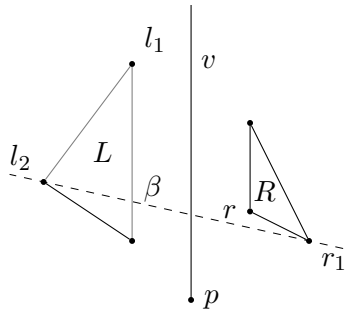

Figure 6: Angle-instance with $n = 7$: Construction of an optimal tour: phase 2.

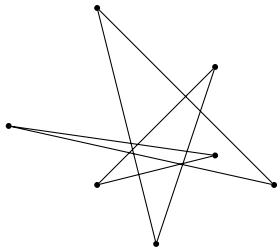

Figure 7: Angle-instance with $n = 7$: Optimal MaxAngle TSP tour.

the data structure of Hershberger and Suri supports binary search [16, p. 254], one can apply an algorithm by Guibas, Hershberger, and Snoeyink [14, Lemma A.1] to find the counterclockwise bitangent in $O(\log n)$ time in each iteration. □

We remark that the proof is inspired by the technique used in [1, Theorem 3.1], where bitangents with both subsets on the same side are used for creating a plane path that alternates between the two subsets.

5.1.2 MaxAngle TSP: n is even

Lemma 6. *Let $G = (V, A)$ be an instance of MaxAngle TSP. If n is even, then for every optimal tour T^* there is:*

$$0 \leq \widehat{f}(G, T^*) \leq 2\pi. \tag{27}$$

Proof. The lower bound is trivial. To show the upper bound we apply the algorithm described in Section 5.1.1 after removing an arbitrary vertex q to obtain a tour $\tilde{T}$ on $V \setminus \{q\}$. Pick an arbitrary edge ij of $\tilde{T}$ and replace it by the edges iq and qj, obtaining a tour T on V. The reverse objective value for $\tilde{T}$ was π, and $\tilde{T}$ and T only differ in the angles at i, j and q. The sum of the changes in these three inner angles is the angle sum of the triangle ijq, which is π. Hence, the reverse objective value for T can increase by at most π, and so we get an upper bound of 2π. (Observe that this increase may be less than π if, say, the edge jk of $\tilde{T}$, $k \neq i$, intersects the interior of the triangle ijq.) □

Note that the lower bound can be reached trivially by an instance where all vertices lie on a line. The following result shows that also the upper bound is tight.

Theorem 7. *Let $G = (V, A)$ be an instance of MaxAngle TSP with n vertices corresponding to n equally placed points on the unit circle. Then for n even every solution T fulfills*

$$\widehat{f}(G, T) \geq \frac{2(n-2)}{n} \cdot \pi. \tag{28}$$

Proof. Let n be even. For convenience denote $V = \{0, \ldots, n-1\}$ and let vertex $u \in V$ be embedded in the plane at point $(\cos(2\pi\frac{u}{n}), \sin(2\pi\frac{u}{n})) \in \mathbb{R}^2$. Consider an arbitrary tour T in G.

Let $C = (0, 1, 2, \ldots, n-1)$ be the canonical cycle in G and denote by $d_C(u, v)$ the length of the shortest path (number of edges) between u and v in C. Now consider any three

successive vertices u, v, w on the tour T: Observe that the inner angle $\widehat{\alpha}_{uvw}$ at v is at least $d_C(u,w) \cdot \frac{\pi}{n}$ because the central angles between u and w are $\frac{2\pi}{n} d_C(u,w)$ and $2\pi - \frac{2\pi}{n} d_C(u,w)$, hence the inscribed angles are $\frac{\pi}{n} d_C(u,w)$ and $\pi - \frac{\pi}{n} d_C(u,w)$. Therefore, it suffices to prove that for each tour $T = (u_0, u_1, \ldots, u_{n-1})$ the following inequality is satisfied,

$$\ell(T) := \sum_{i=0}^{n-1} d_C(u_i, u_{(i+2) \bmod n}) \geq 2 \cdot (n-2).$$

The tour T defines two subtours $T_1 = (u_0, u_2, \ldots, u_{n-2})$ and $T_2 = (u_1, u_3, \ldots, u_{n-1})$ on the even and odd numbered vertices of T, respectively. In particular, the value $\ell(T)$ of tour T is exactly the sum of the lengths of T_1 and T_2 w. r. t. the edge lengths d_C, i. e., with $d_C(T_i)$ denoting the sum of the edge weights of T_i, $i = 1, 2$,

$$\ell(T) = d_C(T_1) + d_C(T_2). \tag{29}$$

Now observe that there must be two vertices u_i, u_j, $i, j \in \{0, 2, \ldots, n-2\}$ with $d_C(u_i, u_j) \geq \frac{n}{2} - 1$: if there are two vertices $u_i = k, u_j = k + \frac{n}{2} \in V(T_1)$ for some $k \in \{0, \ldots, \frac{n}{2} - 1\}$ then $d_C(u_i, u_j) = \frac{n}{2}$. Otherwise, by the pigeonhole principle, we know that for all $k \in \{0, \ldots, \frac{n}{2} - 1\}$ either $k \in V(T_1)$ or $(k + \frac{n}{2}) \in V(T_1)$. So choose $k' \in \{0, \ldots, n-1\}$ with $k' \in V(T_1)$ and $((k'+1) \bmod n) \notin V(T_1)$, then for $u_i = k'$ and $u_j = (k' + 1 + \frac{n}{2}) \bmod n$ we have $d_C(u_i, u_j) = \frac{n}{2} - 1$.

The triangle inequality implies $d_C(T_1) \geq 2 \cdot d_C(u_i, u_j) \geq 2 \cdot (\frac{n}{2} - 1) = n - 2$ and, analogously, $d_C(T_2) \geq n - 2$. Hence (29) shows $\ell(T) \geq 2 \cdot (n-2)$. □

So, for the instances considered in Theorem 7 the lower bound on the optimal reverse objective value $\widehat{f}(G,T)$ tends to 2π for $n \to \infty$.

Remark 8. *Considering the instances in Theorem 7, the optimal value $2 \cdot (n-2) \cdot \frac{\pi}{n}$ is attained by a large number of different tours. In fact, it can be shown that $2^{n-7}n^2$ optimal solutions for the MaxAngle TSP exist in this case. Note that it follows from the proof of Theorem 7 that a half tour T_1 can have length $n-2$ if and only if it covers exactly $\frac{n}{2}$ consecutive vertices, say $\{u_0, u_2, \ldots, u_{n-2}\} = \{0, 1, \ldots, \frac{n}{2} - 1\}$. (In this case, we know that $\widehat{\alpha}_{uvw}$ actually equals $d_C(u,w) \cdot \frac{\pi}{n}$.) In particular, T_1 must satisfy, w. l. o. g.,*

- *$u_0 = 0$, $u_{\hat{\imath}} = \frac{n}{2} - 1$ for some $\hat{\imath} \in \{0, 2, \ldots, n-2\}$,*
- *$u_i < u_j$ for all $0 \leq i < j \leq \hat{\imath}$,*
- *$u_i > u_j$ for all $\hat{\imath} \leq i < j \leq \frac{n}{2} - 1$.*

This gives, for fixed "turning vertices" $\{0, \frac{n}{2} - 1\}$, exactly $2^{\frac{n}{2}-2}/2$ tours (because each tour can be traversed in both directions). The same number of tours is possible for T_2. Furthermore, note that T_2 can be combined with T_1 by starting with u_0 of T_1 and an arbitrary vertex $u_{2i+1}, i \in \{1, 3, \ldots, n-1\}$, of T_2 and with T_2 being traversed in both directions, giving $2 \cdot \frac{n}{2} = n$ possible combinations. Finally there are $\frac{n}{2}$ possible choices for the turning vertices of T_1. Putting all together we can construct exactly

$$\left(\frac{2^{\frac{n}{2}-2}}{2}\right)^2 \cdot \frac{n}{2} \cdot n = 2^{n-7}n^2$$

optimal tours.

It should be noted that the equidistant points on a unit circle do not seem to be the worst case instances for the reverse objective value of MaxAngle TSP. For $n = 4$ and $n = 6$ we could reach higher values for instances where we arrange $n-1$ vertices equally distributed along the unit circle and one vertex at the center of this circle. It is open, how worst case instances for $n \geq 8$ look like.

5.2 Computational results for MaxSQTSP

We now consider the different instance classes for the MaxSQTSP from a computational point of view. The results are summarized in Tables 5 and 6 in the Appendix. They both use the elementary fractional approach (column F) as the reference method and thus the ratios in the remaining columns are comparable. In particular, Table 5 contains the results for all methods based on the fractional and Table 6 for the integral separation process, respectively. As we have seen in Sections 5.1.1 and 5.1.2, the MaxAngle TSP behaves very differently in the odd and in the even case from a theoretical point of view. Thus, we evaluated the Angle- and Angle-Distance-instances separately for n even and n odd, respectively, in our tables.

Angle-instances, n even: Similar to the minimization problems, all introduced integral approaches beat their fractional counterparts. However, different from the minimization case, the stronger subtour elimination constraints do improve the performance in the case of maximization. All the methods F(III)/I(III), F(IV)/I(IV) and F(V)/I(V) beat the *elementary integral approach*. Moreover, the methods F(IV)/I(IV) lie between the *elementary approaches* and the variants F(III)/I(III) as one could expect from a theoretical point of view (for details see Section 4.1). The best approach among all is I(III) for this instance type.

Angle-instances, n odd: As already proved in Section 5.1.1, the inclusion of subtour elimination constraints is not necessary to solve these instances (at least for points in non-collinear position). However, some subtour elimination constraints can be separated inside the branch and cut tree during the solution process. Consequently, we can observe different solution times caused by the particular methods. The *elementary fractional approach* performs as well as the *elementary integral approach* and among all tested approaches, the method F(III) outperforms the other ones significantly. Contrary to the even case, the variants (II) and (IV) seem to slow down the solution process.

Angle-Distance-instances, n even: The methods F(III)/I(III) and F(V)/I(V) yield the best running times in this case, similarly as for the Angle-instances with n even. We can also observe that the integral approaches outperform their fractional counterparts with the notable exceptions of methods I(II) and I(IV) which surprisingly perform extremely poor. Although the entries greater than 20 are always caused by one single outlier instance, also the other ratios are quite high. The overall best running times for this instance type are derived with the methods I(III) and I(V), where I(III) slightly outperforms I(V).

Angle-Distance-instances, n odd: For these instances, the trends are less clear. We can see that even the absolute running times in the first column do not increase monotonically and similar variances can be observed in other columns. Looking at all the table entries and not only the mean values, the method F(III) provides the best performance. Moreover, apart from the methods F(V)/I(V) the fractional approaches outperform their integral counterparts.

A rather surprising observation shows that many instances yield the same optimal tour as it would be obtained by solving the corresponding Angle-instances on the same point sets. Of course, the optimization goals of maximizing the turning angles and the distances are not contradictory, but we could observe that even for $\rho = 0$ we often got an optimal MaxAngle TSP tour. For these instances, the optimal tour does not change by increasing ρ, however, a significant increase of the running time occurs for larger values of ρ.

Random-instances: Finally, the integral methods mostly beat their fractional counterparts for Random-instances. The methods I(II) and I(IV) yield the best running times, although I(I) and I(III) do not lag far behind.

Summing up the results for the maximization problem we cannot identify a clear winner for all instance classes. Different from the minimization case, the variants of stronger subtour elimination constraints improve the performance in many cases. In particular, the stronger subtour elimination constraints (III) improve the performance for all angle-based test instances. However, for both the Angle- and Angle-Distance-instance classes

- the integral approach outperforms the fractional one if n is even and
- the fractional approach outperforms the integral one if n is odd.

If forced to nominate one method of choice our pick would be I(III).

6 Conclusions

In this paper we deal with the *symmetric quadratic traveling salesman problem* (*SQTSP*) and two geometric variants, namely the *Angular-Metric Traveling Salesman Problem* (*Angle TSP*) where the distances correspond to the *turning angles* of the tour, and the *Angular-Distance Metric Traveling Salesman Problem* (Angle-Distance TSP) where turning angles are combined with Euclidean distances. Moreover, we introduce the maximization variants MaxSQTSP and MaxAngle TSP, which were not treated in the literature before.

Contributing to ILP-based solution approaches, we consider a standard linearization and test a purely integral subtour elimination process. This basic approach turns out to significantly outperform the standard fractional separation procedure known from the literature for all types of test instance types in all problem variants. Note that such a behavior does not apply to the classical TSP. After that we include other kinds of subtour elimination constraints [11] in the separation process. Although stronger from a theoretical point of view, for the minimization case the use of these constraints tends to increase the solution times as more non-zero entries are contained in the constraint matrix.

We also introduce a completely new, geometrically based MILP linearization for the Angle TSP and Angle-Distance TSP involving only a linear number of additional variables while the standard linearization requires a cubic number. This approach helps to reduce the running times for Angle-Distance-instances with up to 55 vertices. The downside of this approach are larger root node gaps which may be the reason for worse running times of this approach for large n.

In the second part of the paper we deal with the MaxSQTSP. From a computational point of view, in the maximization case, different from the minimization case, some of the additional constraints speed up the solution process in many cases. The comparison between purely integral and fractional subtour elimination is less clear and depends on the particular type of test instances. It also turns out that for geometrically based test instances a dramatic difference between the cases of even and odd number of vertices can be observed which led us to interesting theoretical results.

If n is odd we can show for MaxAngle TSP by a geometric argument that the reverse optimal objective value (sum of inner turning angles) is always equal to π. Geometrically, given an odd point set there always exists a closed polygonal chain such that the inner angles sum to π. This also implies that the solution of the standard ILP model will never produce subtours and so integral separation does not occur at all. Even though, the solution times for this simple ILP increase dramatically for the maximization case. But fortunately, we

provide a simple constructive polynomial time algorithm to find such an optimal solution. In contrary, if n is even it can be shown that the reverse objective function value lies between 0 and 2π and that these bounds are tight. The latter is shown by an analytic solution of the MaxAngle TSP for a regular n-gon. Note that the complexity status of MaxAngle TSP for n even remains an open question.

Acknowledgments

The research was funded by the Austrian Science Fund (FWF): P 23829-N13. O. A. and A. P. were partially supported by the ESF EUROCORES programme EuroGIGA – CRP ComPoSe, Austrian Science Fund (FWF): I 648-N18.

References

[1] M. Abellanas, J. Garcia-Lopez, G. Hernández-Peñalver, M. Noy, and P. A. Ramos. Bipartite embeddings of trees in the plane. *Discrete Applied Mathematics*, 93(2-3): 141–148, 1999.

[2] A. Aggarwal, D. Coppersmith, S. Khanna, R. Motwani, and B. Schieber. The angular-metric traveling salesman problem. *SIAM Journal on Computing*, 29(3):697–711, 2000.

[3] E. Amaldi, G. Galbiati, and F. Maffioli. On minimum reload cost paths, tours, and flows. *Networks*, 57(3):254–260, 2011.

[4] D. L. Applegate, R. E. Bixby, V. Chvátal, and W. J. Cook. *The Traveling Salesman Problem: A Computational Study.* Princeton University Press, 2006.

[5] J. Beardwood, J. H. Halton, and J. M. Hammersley. The shortest path through many points. *Mathematical Proceedings of the Cambridge Philosophical Society*, 55(4):299–327, 1959.

[6] G. Dantzig, R. Fulkerson, and S. Johnson. Solution of a large-scale traveling-salesman problem. *Journal of the Operations Research Society of America*, 2(4):393–410, 1954.

[7] S. S. Dey, M. Molinaro, and Q. Wang. How good are sparse cutting-planes? In *Proceedings of the 17th International Conference on Integer Programming and Combinatorial Optimization, IPCO*, volume 8494 of *Lecture Notes in Computer Science*, pages 261–272. Springer, 2014.

[8] A. Dumitrescu, J. Pach, and G. Tóth. Drawing Hamiltonian cycles with no large angles. *Electronic Journal of Combinatorics*, 19(2):P31, 2012.

[9] S. P. Fekete and G. J. Woeginger. Angle-restricted tours in the plane. *Computational Geometry*, 8(4):195–218, Sept. 1997.

[10] A. Fischer. *A Polyhedral Study of Quadratic Traveling Salesman Problems.* PhD thesis, Chemnitz University of Technology, Department of Mathematics, 2013. Available at: `http://www.qucosa.de/fileadmin/data/qucosa/documents/11834/Dissertation_Anja_Fischer.pdf`.

[11] A. Fischer and C. Helmberg. The symmetric quadratic traveling salesman problem. *Mathematical Programming A*, 142(1):205–254, 2013.

[12] A. Fischer, F. Fischer, G. Jäger, J. Keilwagen, P. Molitor, and I. Grosse. Exact algorithms and heuristics for the quadratic traveling salesman problem with an application in bioinformatics. *Discrete Applied Mathematics*, 166:97–114, 2014.

[13] G. Galbiati, S. Gualandi, and F. Maffioli. On minimum reload cost cycle cover. *Discrete Applied Mathematics*, 164, Part 1:112–120, 2014.

[14] L. J. Guibas, J. Hershberger, and J. Snoeyink. Compact interval trees: a data structure for convex hulls. *International Journal of Computational Geometry & Applications*, 1 (1):1–22, 1991.

[15] G. Gutin and A. P. Punnen, editors. *The Traveling Salesman Problem and Its Variations*, volume 12 of *Combinatorial Optimization*. Springer US, 2007.

[16] J. Hershberger and S. Suri. Applications of a semi-dynamic convex hull algorithm. *BIT Numerical Mathematics*, 32(2):249–267, 1992.

[17] G. Jäger and P. Molitor. Algorithms and experimental study for the traveling salesman problem of second order. In *Proceedings of COCOA*, volume 5165 of *Lecture Notes in Computer Science*, pages 211–224. Springer, 2008.

[18] E. L. Lawler, J. K. Lenstra, A. H. G. Rinnooy Kan, and D. B. Shmoys, editors. *The Traveling Salesman Problem: A Guided Tour of Combinatorial Optimization*. Wiley-Interscience Series in Discrete Mathematics and Optimization, 1985.

[19] J. F. Meier and U. Clausen. Solving classical and new single allocation hub location problems on Euclidean data, 2015. Available as: Optimization Online 2015-03-4816.

[20] U. Pferschy and R. Staněk. Generating subtour elimination constraints for the TSP from pure integer solutions. *Central European Journal of Operations Research*, to appear, 2016. doi: 10.1007/s10100-016-0437-8. Available as: `arXiv:1511.03533`.

[21] G. Reinelt. *The Traveling Salesman: Computational Solutions for TSP Applications*. Springer, 1994.

[22] K. Savla, E. Frazzoli, and F. Bullo. Traveling salesperson problems for the Dubins vehicle. *IEEE Transactions on Automatic Control*, 53(6):1378–1391, 2008.

A Appendix

We refer to Section 3 for a detailed description of the structure of all tables comparing the particular approaches. In general, the first column always contains the absolute running times of a reference method in seconds. The other columns report the ratios between the particular running times and the running times of the reference method. *Means* report arithmetic means if absolute running times are considered, and geometric means if ratios are considered. Finally, since we created 10 test instances for every instance type and size, we report only the mean values in every row.

Instance	**I (constr. (7))**	**I (constr. (12))**	**I (constr. (13))**
Angle_25	1.3	1.11	1.11
Angle_30	3.3	1.01	1.01
Angle_35	6.6	1.08	1.08
Angle_40	57.9	1.06	1.06
Angle_45	129.1	1.12	1.12
Angle_50	321.3	1.00	1.00
Angle_55	1099.8	1.07	1.07
mean		*1.07*	*1.07*
Angle-Distance_50	19.2	0.98	0.98
Angle-Distance_55	80.6	1.02	1.02
Angle-Distance_60	68.5	1.01	1.01
Angle-Distance_65	104.3	1.10	1.08
Angle-Distance_70	543.4	1.01	1.01
Angle-Distance_75	773.2	0.98	0.98
Angle-Distance_80	1719.5	0.95	0.95
mean		*1.00*	*1.00*
Random_20	3.8	0.97	1.05
Random_25	34.2	1.12	1.05
Random_30	331.4	0.82	0.83
Random_35	2979.1	1.03	0.92
mean		*0.98*	*0.96*

Table 1: Minimization case: comparing the running times of the approaches I (subtour elimination constraints as in (7)), I (subtour elimination constraints as in (12)) and the elementary integral approach I (subtour elimination constraints as in (13)).

Instance	**F**	**F$^{\mathrm{L}}$**	**I**	**I$^{\mathrm{L}}$**	**ratio**	**ratio$^{\mathrm{L}}$**
Angle_25	1.6	1.55	0.91	1.30	0.91	0.89
Angle_30	3.7	1.98	0.95	1.72	0.92	0.90
Angle_35	7.7	3.39	0.92	2.77	0.91	0.88
Angle_40	63.9	5.30	0.98	4.03	0.91	0.86
Angle_45	148.1	10.02	0.84	9.12	0.90	0.86
Angle_50	443.9	Ø	0.81	Ø	0.91	Ø
Angle_55	2183.3	Ø	0.86	Ø	0.91	Ø
mean		*3.53*	*0.89*	*2.96*	*0.91*	*0.88*
Angle-Distance_30	0.8	0.59	1.04	0.56	0.98	0.97
Angle-Distance_35	2.3	0.53	0.96	0.43	0.97	0.96
Angle-Distance_40	3.4	0.60	0.90	0.53	0.97	0.96
Angle-Distance_45	11.8	0.75	0.95	0.51	0.96	0.95
Angle-Distance_50	22.4	0.76	0.84	0.47	0.95	0.95
Angle-Distance_55	85.7	0.93	0.92	0.61	0.95	0.94
Angle-Distance_60	80.3	1.36	0.87	1.00	0.95	0.94
Angle-Distance_65	126.7	2.07	0.84	1.36	0.95	0.94
Angle-Distance_70	909.1	1.91	0.67	1.28	0.95	0.94
Angle-Distance_75	1035.8	4.55	0.77	3.11	0.95	0.93
Angle-Distance_80	3742.4	6.46[a]	0.60	3.91	0.95	0.93
mean		*1.27*	*0.84*	*0.92*	*0.96*	*0.95*
Random_20	4.6	–	0.90	–	0.66	–
Random_25	41.1	–	0.87	–	0.64	–
Random_30	306.1	–	0.90	–	0.63	–
Random_35	2990.1	–	0.81	–	0.62	–
mean		–	*0.87*	–	*0.64*	–

Table 2: Minimization case: comparing the running times of the elementary fractional approach F, the approach F$^{\mathrm{L}}$, the elementary integral approach I and the approach I$^{\mathrm{L}}$. Moreover, the table compares the respective root node ratios (i. e., the ratio between root node value of the LP-relaxation and optimal solution value) of the two linearizations in columns *ratio* and *ratio*$^{\mathrm{L}}$.

[a] Mean of 9 instances (one instance did not fit into 16 GB RAM).

Instance	**F**	**F(I)**	**F(II)**	**F(III)**	**F(IV)**	**F(V)**
Angle_25	1.6	1.07	1.03	1.03	1.14	1.02
Angle_30	3.7	1.00	1.01	1.04	1.00	1.08
Angle_35	7.7	0.99	1.01	1.07	0.98	1.14
Angle_40	63.9	1.03	1.07	1.10	1.08	1.14
Angle_45	148.1	0.99	0.90	1.00	1.04	1.03
Angle_50	443.9	0.97	1.14	1.03	1.05	1.14
Angle_55	2183.3	1.03	1.06	1.06	1.00	1.12
mean		*1.01*	*1.03*	*1.05*	*1.04*	*1.09*
Angle-Distance_50	22.4	1.00	1.03	0.97	0.93	0.90
Angle-Distance_55	85.7	1.02	0.95	1.30	1.04	1.03
Angle-Distance_60	80.3	1.06	0.98	1.13	1.02	0.98
Angle-Distance_65	126.7	1.02	1.02	1.13	0.89	1.04
Angle-Distance_70	909.1	1.02	1.07	1.13	0.98	1.05
Angle-Distance_75	1035.8	1.05	1.15	1.43	1.21	1.13
Angle-Distance_80	3742.4	0.93	0.90	1.22	0.93	0.99
mean		*1.01*	*1.01*	*1.18*	*0.99*	*1.01*
Random_20	4.6	0.86	0.79	0.89	0.92	0.87
Random_25	41.1	0.76	0.94	0.92	0.89	0.82
Random_30	306.1	1.12	1.10	1.09	0.87	1.01
Random_35	2990.1	0.98	1.11	1.13	1.11	1.07
mean		*0.92*	*0.98*	*1.00*	*0.94*	*0.94*

Table 3: Minimization case: comparing the running times of the elementary fractional approach F and other fractional approaches using different variants of subtour elimination constraints.

Instance	**I**	**I(I)**	**I(II)**	**I(III)**	**I(IV)**	**I(V)**
Angle_25	1.4	1.08	1.01	1.10	1.13	1.03
Angle_30	3.4	1.01	1.03	1.04	1.04	1.07
Angle_35	6.8	1.04	1.04	1.06	1.00	1.17
Angle_40	59.5	0.95	0.98	0.95	0.99	1.09
Angle_45	125.7	1.04	1.02	1.07	1.04	1.15
Angle_50	323.1	1.11	1.12	0.96	1.09	1.23
Angle_55	1299.2	0.94	0.92	1.00	1.05	1.22
mean		*1.02*	*1.02*	*1.02*	*1.05*	*1.13*
Angle-Distance_50	19.1	1.11	1.26	1.02	1.10	1.14
Angle-Distance_55	78.2	0.94	1.13	1.12	1.09	1.25
Angle-Distance_60	70.4	0.92	1.04	0.90	0.97	0.97
Angle-Distance_65	102.6	1.01	1.14	1.09	1.13	1.08
Angle-Distance_70	444.7	1.13	1.55	1.17	1.40	1.26
Angle-Distance_75	784.1	0.98	0.94	1.07	0.96	1.10
Angle-Distance_80	1699.2	0.99	0.96	1.00	0.98	1.03
mean		*1.01*	*1.13*	*1.05*	*1.08*	*1.11*
Random_20	3.9	0.99	0.97	0.90	0.88	0.91
Random_25	37.0	0.76	0.88	0.82	0.92	0.79
Random_30	235.3	0.97	1.15	1.35	1.05	1.27
Random_35	2887.0	1.07	1.04	1.07	1.07	1.37
mean		*0.94*	*1.00*	*1.01*	*0.98*	*1.06*

Table 4: Minimization case: comparing the running times of the elementary integral approach I and other integral approaches using different variants of subtour elimination constraints.

Instance	**F**	**F(I)**	**F(II)**	**F(III)**	**F(IV)**	**F(V)**
Angle_10	0.1	0.99	1.01	0.98	0.95	0.85
Angle_12	1.2	0.96	1.04	0.80	0.88	0.80
Angle_14	6.2	1.04	0.95	0.75	0.95	0.72
Angle_16	263.2	0.89	0.94	0.49	1.03	0.59
Angle_18	4270.8	0.97	1.16	0.38	0.98	0.57
mean		*0.97*	*1.02*	*0.65*	*0.96*	*0.70*
Angle_11	0.3	1.02	0.99	0.91	0.98	0.83
Angle_13	1.1	1.17	1.25	0.93	0.98	0.92
Angle_15	7.3	0.95	1.02	0.69	0.92	0.85
Angle_17	22.9	0.79	1.20	0.82	1.34	1.10
Angle_19	254.1	1.05	1.24	0.41	1.08	0.90
mean		*0.99*	*1.13*	*0.72*	*1.05*	*0.92*
Angle-Distance_16	0.8	0.98	1.00	0.94	1.01	0.97
Angle-Distance_18	1.3	0.99	1.07	0.81	1.04	0.95
Angle-Distance_20	2.8	0.98	1.02	0.56	1.09	0.83
Angle-Distance_22	24.4	0.86	0.89	0.41	0.86	0.55
Angle-Distance_24	50.0	0.97	0.92	0.44	1.18	0.63
Angle-Distance_26	304.8	0.85	1.10	0.42	1.19	0.62
mean		*0.94*	*1.00*	*0.56*	*1.06*	*0.74*
Angle-Distance_41	4.8	0.99	0.98	0.78	1.04	1.02
Angle-Distance_43	5.3	0.94	0.93	0.70	0.91	0.91
Angle-Distance_45	17.3	0.95	0.86	0.51	0.96	0.71
Angle-Distance_47	6.3	1.02	1.06	0.68	0.93	0.86
Angle-Distance_49	16.1	1.21	1.17	0.77	1.18	1.02
Angle-Distance_51	17.7	0.86	0.91	0.45	0.97	0.98
Angle-Distance_53	39.3	1.03	1.05	0.60	0.99	1.00
Angle-Distance_55	32.1	0.91	0.96	0.60	0.81	0.85
Angle-Distance_57	74.2	1.04	0.99	0.42	0.96	1.14
Angle-Distance_59	325.7	0.86	0.74	0.33	0.86	0.78
Angle-Distance_61	63.4	1.11	0.94	0.59	1.00	0.97
Angle-Distance_63	107.7	1.00	0.90	0.48	0.84	0.78
Angle-Distance_65	257.6	0.84	0.99	0.32	0.86	0.77
mean		*0.98*	*0.95*	*0.54*	*0.94*	*0.90*
Random_20	4.1	0.95	0.94	1.02	0.93	1.04
Random_25	39.8	0.90	1.02	1.01	0.75	0.92
Random_30	425.0	0.77	0.87	0.89	0.70	0.97
Random_35	3911.1	0.88	1.15	1.11	0.75	0.91
mean		*0.87*	*0.99*	*1.00*	*0.78*	*0.96*

Table 5: Maximization case: comparison of the running times. We compare the elementary fractional approach F with fractional approaches using different variants of subtour elimination constraints.

Instance	**F**	**I**	**I(I)**	**I(II)**	**I(III)**	**I(IV)**	**I(V)**
Angle_10	0.1	0.95	0.95	0.97	0.96	0.96	0.83
Angle_12	1.2	0.95	0.97	1.05	0.77	0.86	0.75
Angle_14	6.2	0.86	0.84	1.12	0.69	0.96	0.71
Angle_16	263.2	0.62	0.58	1.04	0.44	1.04	0.49
Angle_18	4270.8	0.40	0.32	0.62	0.33	0.72	0.42
mean		*0.72*	*0.68*	*0.94*	*0.59*	*0.90*	*0.62*
Angle_11	0.3	0.97	0.94	0.93	0.92	0.90	0.81
Angle_13	1.1	1.00	0.96	1.16	1.01	1.11	0.84
Angle_15	7.3	0.92	0.77	1.02	0.83	1.04	0.92
Angle_17	22.9	1.34	1.08	1.34	0.92	1.23	0.97
Angle_19	254.1	0.83	0.79	0.88	0.69	0.89	0.72
mean		*1.00*	*0.90*	*1.05*	*0.87*	*1.03*	*0.85*
Angle-Distance_16	0.8	1.05	0.98	1.64	0.93	1.69	0.99
Angle-Distance_18	1.3	1.03	1.11	2.28	0.79	2.20	0.73
Angle-Distance_20	2.8	1.07	1.02	5.91	0.61	4.73	0.62
Angle-Distance_22	24.4	0.69	0.65	22.31	0.33	21.24	0.44
Angle-Distance_24	50.0	0.84	0.69	9.04	0.46	8.57	0.48
Angle-Distance_26	304.8	0.73	0.59	20.80	0.37	12.65	0.45
mean		*0.89*	*0.81*	*6.73*	*0.54*	*5.86*	*0.59*
Angle-Distance_41	4.8	1.16	1.20	1.30	0.91	1.35	1.11
Angle-Distance_43	5.3	1.03	1.01	0.88	0.99	0.96	1.10
Angle-Distance_45	17.3	0.98	1.04	0.96	0.74	1.27	0.99
Angle-Distance_47	6.3	1.16	1.19	1.11	0.86	1.11	0.91
Angle-Distance_49	16.1	1.13	1.22	1.27	1.11	1.24	1.06
Angle-Distance_51	17.7	1.03	1.08	0.96	0.62	1.10	0.81
Angle-Distance_53	39.3	1.26	0.97	1.29	0.89	1.18	0.89
Angle-Distance_55	32.1	0.82	0.96	0.83	0.80	1.02	0.82
Angle-Distance_57	74.2	1.32	1.27	1.19	0.71	1.45	0.83
Angle-Distance_59	325.7	0.90	0.98	1.05	0.60	0.77	0.69
Angle-Distance_61	63.4	0.94	0.89	0.87	0.71	1.01	0.82
Angle-Distance_63	107.7	1.16	1.13	1.24	0.75	1.45	0.93
Angle-Distance_65	257.6	0.80	0.85	0.77	0.51	0.69	0.60
mean		*1.04*	*1.05*	*1.04*	*0.77*	*1.10*	*0.88*
Random_20	4.1	0.81	0.93	0.85	0.86	0.83	0.98
Random_25	39.8	0.80	0.90	0.64	0.89	0.73	0.88
Random_30	425.0	0.86	0.72	0.73	0.72	0.74	0.97
Random_35	3911.1	1.02	0.80	0.77	0.87	0.74	0.93
mean		*0.87*	*0.83*	*0.74*	*0.83*	*0.76*	*0.94*

Table 6: Maximization case: comparison of the running times. We compare the elementary integral approach I with the elementary fractional approach F and with integral approaches using different variants of subtour elimination constraints.

Institut für Numerische und Angewandte Mathematik
Universität Göttingen
Lotzestr. 16-18
D - 37083 Göttingen

Telefon: 0551/394512
Telefax: 0551/393944

Email: trapp@math.uni-goettingen.de URL: http://www.num.math.uni-goettingen.de

Verzeichnis der erschienenen Preprints 2016

Number	Authors	Title
2016 - 1	Aichholzer, O., Fischer, A., Fischer, F., Meier, J.F., Pferschy, U., Pilz, A., Stanek, R.	Minimization and Maximization Versions of the Quadratic Traveling Salesman Problem